# Inversion of moments to retrieve joint probabilities in quantum sequential measurements

H. S. Karthik
*Raman Research Institute, Bangalore 560 080, India*

Hemant Katiyar, Abhishek Shukla, and T. S. Mahesh
*Department of Physics and NMR Research Center, Indian Institute of Science Education and Research, Pune 411008, India*

A. R. Usha Devi*
*Department of Physics, Bangalore University, Bangalore 560 056, India and Inspire Institute Inc., Alexandria, Virginia, 22303, USA*

A. K. Rajagopal
*Inspire Institute Inc., Alexandria, Virginia, 22303, USA and Harish-Chandra Research Institute, Chhatnag Road, Jhunsi, Allahabad 211 019, India*

(Received 5 April 2013; published 14 May 2013)

A sequence of moments obtained from statistical trials encodes a classical probability distribution. However, it is well known that an incompatible set of moments arises in the quantum scenario, when correlation outcomes associated with measurements on spatially separated entangled states are considered. This feature, viz., the incompatibility of moments with a joint probability distribution, is reflected in the violation of Bell inequalities. Here, we focus on sequential measurements on a single quantum system and investigate if moments and joint probabilities are compatible with each other. By considering sequential measurement of a dichotomic dynamical observable at three different time intervals, we explicitly demonstrate that the moments and the probabilities are inconsistent with each other. Experimental results using a nuclear magnetic resonance system are reported here to corroborate these theoretical observations, viz., the incompatibility of the three-time joint probabilities with those extracted from the moment sequence when sequential measurements on a single-qubit system are considered.

DOI: 10.1103/PhysRevA.87.052118 PACS number(s): 03.65.Ta, 03.67.Lx

## I. INTRODUCTION

The issue of determining a probability distribution uniquely in terms of its moment sequence, known as the *classical moment problem*, has been developed for more than 100 years [1,2]. In the case of discrete distributions with the associated random variables taking finite values, moments faithfully capture the essence of the probabilities; i.e., the probability distribution is moment determinate [3].

In the special case of classical random variables $X_i$ assuming dichotomic values $x_i = \pm 1$, it is easy to see that the sequence of moments [4] $\mu_{n_1 n_2 \cdots n_k} = \langle X_1^{n_1} X_2^{n_2} \cdots X_k^{n_k} \rangle = \sum_{x_1,x_2,\ldots,x_k=\pm 1} x_1^{n_1} x_2^{n_2} \cdots x_k^{n_k} P(x_1,x_2,\ldots,x_k)$, where $n_1,n_2,\ldots,n_k = 0,1$, can be readily inverted to obtain the joint probabilities $P(x_1,x_2,\ldots,x_k)$ uniquely. More explicitly, the joint probabilities $P(x_1,x_2,\ldots,x_k)$ are given in terms of the $2^k$ moments $\mu_{n_1 n_2 \cdots n_k}, n_1,n_2,\ldots,n_k = 0,1$ as

$$P(x_1,x_2,\ldots,x_k) = \frac{1}{2^k} \sum_{n_1,\ldots,n_k=0,1} {x_1}^{n_1} {x_2}^{n_2} \ldots {x_k}^{n_k} \mu_{n_1 n_2 \ldots n_k}$$
$$= \frac{1}{2^k} \sum_{n_1,\ldots,n_k=0,1} {x_1}^{n_1} {x_2}^{n_2} \ldots {x_k}^{n_k} \times \left\langle X_1^{n_1} X_2^{n_2} \cdots X_2^{n_k} \right\rangle. \quad (1)$$

Does this feature prevail in the quantum scenario? This results in a negative answer as it is well known that the moments associated with measurement outcomes on spatially separated parties are not compatible with the joint probability distribution. This feature reflects itself in the violation of Bell inequalities. In this paper we investigate whether moment indeterminacy persists when we focus on sequential measurements on a single quantum system. We show that the discrete joint probabilities originating in the sequential measurement of a single-qubit dichotomic observable $\hat{X}(t_i) = \hat{X}_i$ at different time intervals are not consistent with the ones reconstructed from the moments. More explicitly, considering sequential measurements of $\hat{X}_1$, $\hat{X}_2$, $\hat{X}_3$, we reconstruct the trivariate joint probabilities $P_\mu(x_1,x_2,x_3)$ based on the set of eight moments $\{\langle \hat{X}_1\rangle, \langle \hat{X}_2\rangle, \langle \hat{X}_3\rangle, \langle \hat{X}_1\, \hat{X}_2\rangle, \langle \hat{X}_2\, \hat{X}_3\rangle, \langle \hat{X}_1\, \hat{X}_3\rangle, \langle \hat{X}_1\, \hat{X}_2\, \hat{X}_3\rangle\}$ and prove that they do not agree with the three-time joint probabilities (TTJP) $P_d(x_1,x_2,x_3)$ evaluated directly based on the correlation outcomes in the sequential measurement of all three observables. Interestingly, the moments and TTJP can be independently extracted experimentally in the Nuclear Magnetic Resonance (NMR) system, demonstrating the difference between moment-inverted three-time probabilities with the ones directly drawn from experiment, in agreement with theory. To obtain TTJP directly we use the procedure of Ref. [5], and to extract moments we extend the Moussa protocol [6] to a set of noncommutating observables. The specifics are given in Sec. IV.

*arutth@rediffmail.com

 

Disagreement between moment-inverted joint probabilities and the ones based on measurement outcomes in turn reflects the inherent inconsistency that the family of all marginal probabilities does not arise from the grand joint probabilities. The nonexistence of a legitimate grand joint probability distribution, consistent with the set of all pairwise marginals, is attributed as the common origin of a wide range of no-go theorems on noncontextuality, locality, and macrorealism in the foundations of quantum theory [7–14]. The absence of a valid grand joint probability distribution in the sequential measurement on a single quantum system is discussed here in terms of its mismatch with moment sequence.

We organize the paper as follows. In Sec. II we begin with a discussion of moment inversion to obtain joint probabilities of three classical random variables assuming dichotomic values $\pm 1$. We proceed in Sec. III to study the quantum scenario with the help of a specific example of sequential measurements of dichotomic observable at three different times on a spin-1/2 system. We show that the TTJP constructed from eight moments do not agree with those originating from the measurement outcomes. Section IV is devoted to reporting experimental results with NMR implementation on an ensemble of spin-1/2 nuclei, demonstrating that moment-constructed TTJP do not agree with those directly extracted. Section V has concluding remarks.

## II. RECONSTRUCTION OF THE JOINT PROBABILITY OF CLASSICAL DICHOTOMIC RANDOM VARIABLES FROM MOMENTS

Let $X$ denote a dichotomic random variable with outcomes $x = \pm 1$. The moments associated with statistical outcomes involving the variable $X$ are given by $\mu_n = \langle X^n \rangle = \sum_{x=\pm 1} x^n\, P(x)$, $n = 0,1,2,3,\ldots$, where $0 \leqslant P(x = \pm 1) \leqslant 1$, $\sum_{x=\pm 1} P(x) = 1$ are the corresponding probabilities. Given the moments $\mu_0$ and $\mu_1$ from a statistical trial, one can readily obtain the probability mass function:

$$P(1) = \tfrac{1}{2}(\mu_0 + \mu_1) = \tfrac{1}{2}(1 + \mu_1),$$
$$P(-1) = \tfrac{1}{2}(\mu_0 - \mu_1) = \tfrac{1}{2}(1 - \mu_1);$$

that is, moments determine the probabilities uniquely.

In the case of two dichotomic random variables $X_1$, $X_2$, the moments

$$\mu_{n_1,n_2} = \left\langle X_1^{n_1}\, X_2^{n_2} \right\rangle = \sum_{x_1=\pm 1, x_2=\pm 1} x_1^{n_1}\, x_2^{n_2}\, P(x_1,x_2),\ n_1,n_2 = 0,1,\ldots$$

encode the bivariate probabilities $P(x_1,x_2)$. Explicitly,

$$\begin{aligned}
\mu_{00} &= \sum_{x_1,x_2=\pm 1} P(x_1,x_2) = P(1,1) + P(1,-1) + P(-1,1) + P(-1,-1) = 1,\\
\mu_{10} &= \sum_{x_1,x_2=\pm 1} x_1\, P(x_1,x_2) = \sum_{x_1=\pm 1} x_1\ P(x_1),\\
&= P(1,1) + P(1,-1) - P(-1,1) - P(-1,-1),\\
\mu_{01} &= \sum_{x_1,x_2=\pm 1} x_2\, P(x_1,x_2) = \sum_{x_2} x_2\, P(x_2)\\
&= P(1,1) - P(1,-1) + P(-1,1) - P(-1,-1),\\
\mu_{11} &= \sum_{x_1,x_2=\pm 1} x_1\, x_2\, P(x_1,x_2) = P(1,1) - P(1,-1) - P(-1,1) + P(-1,-1).
\end{aligned} \tag{2}$$

Note that the moments $\mu_{10}$ and $\mu_{01}$ involve the marginal probabilities $P(x_1) = \sum_{x_2=\pm 1} P(x_1,x_2)$ and $P(x_2) = \sum_{x_1=\pm 1} P(x_1,x_2)$, respectively, and they could be evaluated based on statistical trials drawn independently from the two random variables $X_1$ and $X_2$.

Given the moments $\mu_{00}, \mu_{10}, \mu_{01}, \mu_{11}$, the reconstruction of the probabilities $P(x_1,x_2)$ is straightforward:

$$\begin{aligned}
P(x_1,x_2) &= \frac{1}{4} \sum_{n_1,n_2=0,1} {x_1}^{n_1} {x_2}^{n_2}\, \mu_{n_1\, n_2}\\
&= \frac{1}{4} \sum_{n_1,n_2=0,1} {x_1}^{n_1} {x_2}^{n_2} \left\langle X_1^{n_1}\, X_2^{n_2} \right\rangle.
\end{aligned} \tag{3}$$

Further, a reconstruction of trivariate joint probabilities $P(x_1,x_2,x_3)$ requires the following set of eight moments: $\{\mu_{000} = 1, \mu_{100} = \langle X_1 \rangle, \mu_{010} = \langle X_2 \rangle, \mu_{010} = \langle X_3 \rangle, \mu_{110} = \langle X_1\, X_2 \rangle, \mu_{011} = \langle X_2\, X_3 \rangle, \mu_{101} = \langle X_1\, X_3 \rangle, \mu_{111} = \langle X_1\, X_2\, X_3 \rangle\}$. The probabilities are retrieved faithfully in terms of the eight moments as

$$\begin{aligned}
P(x_1,x_2,x_3) &= \frac{1}{8} \sum_{n_1,n_2,n_3=0,1} x_1^{n_1}\, x_2^{n_2}\, x_2^{n_3}\, \mu_{n_1\, n_2\, n_3}\\
&= \frac{1}{8} \sum_{n_1,n_2,n_3=0,1} x_1^{n_1}\, x_2^{n_2}\, x_2^{n_3} \left\langle X_1^{n_1}\, X_2^{n_2}\, X_3^{n_3} \right\rangle.
\end{aligned} \tag{4}$$

It is implicit that the moments $\mu_{100}, \mu_{010}$, and $\mu_{001}$ are determined through independent statistical trials involving the random variables $X_1, X_2$, and $X_3$ separately; $\mu_{110}, \mu_{011}$, and $\mu_{101}$ are obtained based on the correlation outcomes of $(X_1,X_2)$, $(X_2,X_3)$, and $(X_1,X_3)$, respectively. More specifically, in the classical probability setting there is a tacit underlying assumption that the set of all marginal probabilities $P(x_1),P(x_2),P(x_3),P(x_1,x_2),P(x_2,x_3),P(x_1,x_3)$ is consistent with the trivariate joint probabilities $P(x_1,x_2,x_3)$. This underpinning does not get imprinted automatically in the quantum scenario. Suppose the observables $\hat{X}_1,\hat{X}_2,\hat{X}_3$ are noncommuting and we consider their sequential measurement. The moments $\mu_{100}=\langle\hat{X}_1\rangle,\mu_{010}=\langle\hat{X}_2\rangle$, and $\mu_{001}=\langle\hat{X}_3\rangle$ may be evaluated from the measurement outcomes of dichotomic observables $\hat{X}_1,\hat{X}_2$, and $\hat{X}_3$ independently; the correlated statistical outcomes in the sequential measurements of $(\hat{X}_1,\hat{X}_2),(\hat{X}_2,\hat{X}_3)$, and $(\hat{X}_1,\hat{X}_3)$ allow one to extract the set of moments $\mu_{110}=\langle\hat{X}_1\hat{X}_2\rangle$, $\mu_{011}=\langle\hat{X}_2\hat{X}_3\rangle,\mu_{101}=\langle\hat{X}_1\hat{X}_3\rangle$; further the moment $\mu_{111}=\langle\hat{X}_1\,\hat{X}_2\,\hat{X}_3\rangle$ is evaluated based on the correlation outcomes when all the three observables are measured sequentially. The joint probabilities $P_\mu(x_1,x_2,x_3)$ retrieved from the moments as given in (4) differ from the ones evaluated directly in terms of the correlation outcomes in the sequential measurement of all three observables. We illustrate this inconsistency appearing in the quantum setting in the next section.

### III. QUANTUM THREE-TIME JOINT PROBABILITIES AND MOMENT INVERSION

Let us consider a spin-1/2 system, the dynamical evolution of which is governed by the Hamiltonian

$$\hat{H}=\tfrac{1}{2}\hbar\,\omega\sigma_x. \tag{5}$$

We choose the $z$ component of spin as our dynamical observable:

$$\begin{aligned}\hat{X}_i&=\hat{X}(t_i)=\sigma_z(t_i)\\&=\hat{U}^\dagger(t_i)\,\sigma_z\,\hat{U}(t_i)\\&=\sigma_z\,\cos\omega\,t_i+\sigma_y\,\sin\omega\,t_i,\end{aligned}\tag{6}$$

where $\hat{U}(t_i)=e^{-i\,\sigma_x\,\omega\,t_i/2}=\hat{U}_i$, and we consider sequential measurements of the observable $\hat{X}_i$ at three different times, $t_1=0,t_2=\Delta t,t_3=2\,\Delta t$:

$$\begin{aligned}&\hat{X}_1=\sigma_z,\\&\hat{X}_2=\sigma_z(\Delta t)=\sigma_z\,\cos(\omega\Delta t)+\sigma_y\,\sin(\omega\Delta t),\\&\hat{X}_3=\sigma_z(2\Delta t)=\sigma_z\,\cos(2\omega\Delta t)+\sigma_y\,\sin(2\omega\Delta t).\end{aligned}\tag{7}$$

Note that these three operators are not commuting in general.

The moments $\langle\hat{X}_1\rangle,\langle\hat{X}_2\rangle,\langle\hat{X}_3\rangle$ are readily evaluated to be

$$\begin{aligned}\mu_{100}&=\langle\hat{X}_1\rangle=\mathrm{Tr}[\hat{\rho}_{\rm in}\,\sigma_z]=0,\\\mu_{010}&=\langle\hat{X}_2\rangle=\mathrm{Tr}[\hat{\rho}_{\rm in}\,\sigma_z(\Delta t)]=0,\\\mu_{001}&=\langle\hat{X}_3\rangle=\mathrm{Tr}[\hat{\rho}_{\rm in}\,\sigma_z(2\Delta t)]=0\end{aligned}$$

when the system density matrix is prepared initially in a maximally mixed state $\hat{\rho}_{\rm in}=\mathbb{1}/2$. The probabilities of outcomes $x_i=\pm1$ in the completely random initial state are given by $P(x_i=\pm1)=\mathrm{Tr}[\hat{\rho}_{\rm in}\,\hat{\Pi}_{x_i}]=\frac{1}{2}$, where $\hat{\Pi}_{x_i}=|x_i\rangle\langle x_i|$ is the projection operator corresponding to the measurement of the observable $\hat{X}_i$.

The two-time joint probabilities arising in the sequential measurements of the observables $\hat{X}_i,\hat{X}_j,\ j>i$, are evaluated as follows. The measurement of the observable $\hat{X}_i$ yielding the outcome $x_i=\pm1$ projects the density operator to $\hat{\rho}_{x_i}=\frac{\hat{\Pi}_{x_i}\,\hat{\rho}_{\rm in}\,\hat{\Pi}_{x_i}}{\mathrm{Tr}[\hat{\rho}_{\rm in}\,\hat{\Pi}_{x_i}]}$. Further, a sequential measurement of $\hat{X}_j$ leads to the two-time joint probabilities as

$$\begin{aligned}P(x_i,x_j)&=P(x_i)\,P(x_j|x_i)\\&=\mathrm{Tr}\big[\hat{\rho}_{\rm in}\,\hat{\Pi}_{x_i}\big]\,\mathrm{Tr}\big[\hat{\rho}_{x_i}\,\hat{\Pi}_{x_j}\big]\\&=\mathrm{Tr}\big[\hat{\Pi}_{x_i}\,\hat{\rho}_{\rm in}\,\hat{\Pi}_{x_i}\,\hat{\Pi}_{x_j}\big]\\&=\langle x_i|\,\hat{\rho}_{\rm in}\,|x_i\rangle\,|\langle x_i|x_j\rangle|^2.\end{aligned}\tag{8}$$

We evaluate the two-time joint probabilities associated with the sequential measurements of $(\hat{X}_1,\hat{X}_2)$, $(\hat{X}_2,\hat{X}_3)$, and $(\hat{X}_1,\hat{X}_3)$ explicitly:

$$P(x_1,x_2)=\tfrac{1}{4}\,[1+x_1\,x_2\,\cos(\omega\Delta t)],\tag{9}$$

$$P(x_2,x_3)=\tfrac{1}{4}\,[1+x_2\,x_3\,\cos(\omega\Delta t)],\tag{10}$$

$$P(x_1,x_3)=\tfrac{1}{4}\,[1+x_1\,x_3\,\cos(2\omega\Delta t)].\tag{11}$$

We then obtain two-time correlation moments as

$$\begin{aligned}\mu_{110}=\langle\,\hat{X}_1\hat{X}_2\rangle&=\sum_{x_1,x_2=\pm1}x_1\,x_2\,P(x_1,x_2)\\&=\cos(\omega\Delta t),\end{aligned}\tag{12}$$

$$\begin{aligned}\mu_{011}=\langle\,\hat{X}_2\hat{X}_3\rangle&=\sum_{x_2,x_3=\pm1}x_2\,x_3\,P(x_2,x_3)\\&=\cos(\omega\Delta t),\end{aligned}\tag{13}$$

$$\begin{aligned}\mu_{101}=\langle\,\hat{X}_1\hat{X}_3\rangle&=\sum_{x_1,x_3=\pm1}x_1\,x_3\,P(x_1,x_3)\\&=\cos(2\,\omega\Delta t).\end{aligned}\tag{14}$$

Further, the three-time joint probabilities $P(x_1,x_2,x_3)$ arising in the sequential measurements of $\hat{X}_1,\hat{X}_2$, followed by $\hat{X}_3$, are given by

$$\begin{aligned}P(x_1,x_2,x_3)&=P(x_1)\,P(x_2|x_1)\,P(x_3|x_1,x_2)\\&=\mathrm{Tr}\big[\hat{\rho}_{\rm in}\,\hat{\Pi}_{x_1}\big]\,\mathrm{Tr}\big[\hat{\rho}_{x_1}\,\hat{\Pi}_{x_2}\big]\,\mathrm{Tr}\big[\hat{\rho}_{x_2}\,\hat{\Pi}_{x_3}\big],\end{aligned}\tag{15}$$

where $\hat{\rho}_{x_2}=\frac{\hat{\Pi}_{x_2}\,\hat{\rho}_{x_1}\,\hat{\Pi}_{x_2}}{\mathrm{Tr}[\hat{\rho}_{x_1}\,\hat{\Pi}_{x_2}]}$. We obtain

$$\begin{aligned}P(x_1,x_2,x_3)&=\mathrm{Tr}\big[\hat{\Pi}_{x_2}\,\hat{\Pi}_{x_1}\,\hat{\rho}_{\rm in}\,\hat{\Pi}_{x_1}\,\hat{\Pi}_{x_2}\,\hat{\Pi}_{x_3}\big]\\&=\langle x_1|\,\hat{\rho}_{\rm in}\,|x_1\rangle\,|\langle x_1|x_2\rangle|^2\,|\langle x_2|x_3\rangle|^2\\&=\frac{P(x_1,x_2)\,P(x_2,x_3)}{\langle x_2|\,\hat{\rho}_{\rm in}\,|x_2\rangle}\\&=\frac{P(x_1,x_2)\,P(x_2,x_3)}{P(x_2)},\end{aligned}\tag{16}$$

where in the third line of (16) we have used (8).

The three-time correlation moment is evaluated to be

$$\begin{aligned}\mu_{111}=\langle\hat{X}_1\,\hat{X}_2\,\hat{X}_3\rangle&=\sum_{x_1,x_2,x_3=\pm1}x_1\,x_2\,x_3\,P(x_1,x_2,x_3)\\&=0.\end{aligned}\tag{17}$$

From the set of eight moments (8), (12), and (17), we construct the TTJP [see (4)] as

$$\begin{aligned} P_\mu(1,1,1) &= \tfrac{1}{8}\,[1+2\cos(\omega\Delta t)+\cos(2\omega\Delta t)] = P_\mu(-1,-1,-1),\\ P_\mu(-1,1,1) &= \tfrac{1}{8}\,[1-\cos(2\omega\Delta t)] = P_\mu(-1,-1,1) = P_\mu(1,1,-1) = P_\mu(1,-1,-1),\\ P_\mu(1,-1,1) &= \tfrac{1}{8}\,[1-2\cos(\omega\Delta t)+\cos(2\omega\Delta t)] = P_\mu(-1,1,-1). \end{aligned} \tag{18}$$

On the other hand, the three dichotomic variable quantum probabilities $P(x_1,x_2,x_3)$ evaluated directly are given by

$$\begin{aligned} P_d(1,1,1) &= \tfrac{1}{8}\,[1+\cos(\omega\,\Delta t)]^2 = P_d(-1,-1,-1),\\ P_d(-1,1,1) &= \tfrac{1}{8}\,[1-\cos^2(\omega\,\Delta t)] = P_d(-1,-1,1) = P_d(1,1,-1) = P_d(1,-1,-1),\\ P_d(1,-1,1) &= \tfrac{1}{8}\,[1-\cos(\omega\,\Delta t)]^2 = P_d(-1,1,-1). \end{aligned} \tag{19}$$

Clearly, there is no agreement between the moment-inverted TTJP (18) and the ones of (19) directly evaluated. In other words, the TTJP realized in a sequential measurement are not invertible in terms of the moments, which in turn reflects the incompatibility of the set of all marginal probabilities with the grand joint probabilities $P_d(x_1,x_2,x_3)$. In fact, it may be explicitly verified that $P(x_1,x_3) \neq \sum_{x_2=\pm 1} P_d(x_1,x_2,x_3)$. Moment indeterminacy points towards the absence of a valid grand probability distribution consistent with all the marginals.

The TTJP and moments can be independently extracted experimentally using NMR methods on an ensemble of spin-1/2 nuclei. The experimental approach and results are reported in the next section.

## IV. EXPERIMENT

The projection operators at time $t=0$ ($\hat{X}_1=\sigma_z$) are $\{\hat{\Pi}_{x_i^0} = |x_i^0\rangle\langle x_i^0|\}_{x_i^0=0,1}$. This measurement basis is rotating under the unitary $\hat{U}_i$, resulting in the time-dependent basis given by $\hat{\Pi}_{x_i^t} = \hat{U}_i^\dagger\,\hat{\Pi}_{x_i^0}\hat{U}_i$. While doing experiments it is convenient to perform the measurement in the computational basis compared to the time-dependent basis. This can be done as follows: We can expand the measurement on an instantaneous state $\rho(t_i)$ as $\hat{\Pi}_{x_i^t}\hat{\rho}(t_i)\hat{\Pi}_{x_i^t} = \hat{U}_i^\dagger\hat{\Pi}_{x_i^0}[\hat{U}_i\hat{\rho}(t_i)\hat{U}_i^\dagger]\Pi_{x_i^0}\hat{U}_i$. Thus, measuring in the time-dependent basis is equivalent to evolving the state under the unitary $\hat{U}_i$, followed by measuring in the computational basis, and finally evolving under the unitary $\hat{U}_i^\dagger$.

The probabilities of measurement outcomes can be encoded onto the ancilla qubits with the help of a controlled-NOT (CNOT) gate (or anti-CNOT gate). To see this property consider a one qubit general state (for the system) and an ancilla in the state $|0\rangle\langle 0|$; the CNOT gate encodes the probabilities as follows:

$$\begin{gathered} (p_0|0\rangle\langle 0| + p_1|1\rangle\langle 1| + a|1\rangle\langle 0| + a^\dagger|0\rangle\langle 1|)_S \otimes |0\rangle\langle 0|_A\\ \downarrow \text{CNOT}\\ |0\rangle\langle 0|_S \otimes p_0|0\rangle\langle 0|_A + |1\rangle\langle 1|_S \otimes p_1|1\rangle\langle 1|_A\\ + |1\rangle\langle 0|_S \otimes a|1\rangle\langle 0|_A + |0\rangle\langle 1|_S \otimes a^\dagger|0\rangle\langle 1|_A. \end{gathered}$$

Now, measuring the diagonal terms of the ancilla qubit, we can retrieve $p_0$ and $p_1$.

We have employed a model as shown in Fig. 1 for measuring TTJP [5]. The grouped gates represent the measurements in the rotated bases. The controlled gates shown can be either CNOT or anti-CNOT gates. We require both CNOT and anti-CNOT gates to perform the "ideal negative result measurement" (INRM) procedure to measure the TTJP noninvasively, as proposed by Knee *et al.* [15]. The idea behind the INRM procedure is as follows: consider a gate which interacts with the ancilla qubit only when the system qubit is in state $|1\rangle$. By applying such a gate we can noninvasively obtain the probability of the measurement outcomes when the system was in the $|0\rangle$ state. Similarly, if we have a gate which can interact with ancilla only if the system qubit is in the $|0\rangle$ state, then we can noninvasively obtain the probability of the measurement outcomes of the system state being in $|1\rangle$. These criteria are fulfilled by the CNOT gate and the anti-CNOT gate, respectively.

The circuit shown in Fig. 1 has two controlled gates for encoding the outcomes of the first and second measurements onto the first and second ancilla qubits, respectively. The third measurement need not be noninvasive since we are not concerned with the further time evolution of the system. A set of four experiments is to be performed, with the following arrangement of the first and second controlled gates for the measurement of the TTJP: (i) CNOT, CNOT; (ii) anti-CNOT, CNOT; (iii) CNOT, anti-CNOT; and (iv) anti-CNOT, anti-CNOT.

The propagators $\hat{U}_i = e^{-i\sigma_x\omega t_i/2}$ are realized by the cascade $\mathbb{H}\hat{U}_d\mathbb{H}$, where $\mathbb{H}$ is the Hadamard gate, and the delay propagator $\hat{U}_d = e^{-i\sigma_z\omega t_i/2}$ corresponds to the $z$ precession of the system qubit at the $\omega = 2\pi\,100$ rad/s resonance offset. The diagonal tomography was performed at the end to determine the probabilities [5].

The three qubits were provided by the three $^{19}$F nuclear spins of trifluoroiodoethylene dissolved in acetone-$d_6$. The structure of the molecule is shown in Fig. 2(a), and the chemical shifts and the scalar coupling values (in Hz) are shown in Fig. 2(b). The effective $^{19}$F spin-lattice ($T_2^*$) and

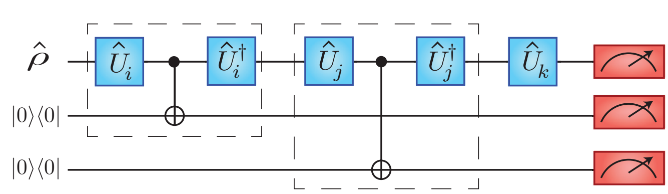


FIG. 1. (Color online) Circuit for finding three-time probability. Grouped gates represent measurement in the rotated basis, and controlled gates can be CNOT or anti-CNOT, as explained in the text.

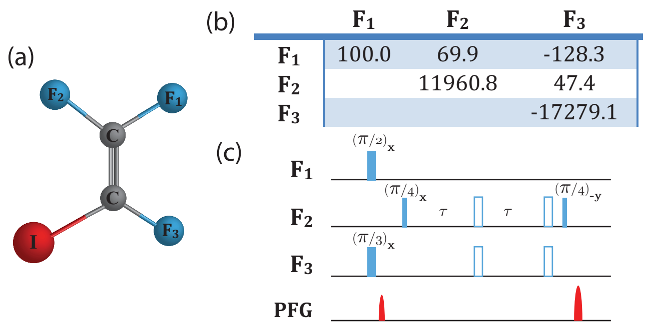


| | $F_1$ | $F_2$ | $F_3$ |
|---|---|---|---|
| $F_1$ | 100.0 | 69.9 | -128.3 |
| $F_2$ | | 11960.8 | 47.4 |
| $F_3$ | | | -17279.1 |

FIG. 2. (Color online) (a) The molecular structure of trifluoroiodoethylene, (b) the corresponding chemical shifts and $J$-coupling values (in Hz), and (c) the pulse sequence for the preparation of initial state. The open pulses are $\pi$ pulses and $\tau = 1/(4J_{23})$.

spin-spin ($T_1$) relaxation time constants were about 0.8 and 6.3 s, respectively. The experiments were carried out at an ambient temperature of 290 K on a 500-MHz Bruker UltraShield NMR spectrometer. The first spin ($F_1$) is used as the system qubit, and the other spins ($F_2$ and $F_3$) are used as the ancilla qubits. Initialization involved preparing the state $\frac{1-\epsilon}{8}\mathbb{1} + \epsilon\{\frac{1}{2}\mathbb{1}_S \otimes |00\rangle\langle 00|_A\}$, where $\epsilon \sim 10^{-5}$ is the purity factor [16]. The pulse sequence to prepare this state from the equilibrium state is shown in Fig. 2(c). All pulses were numerically optimized using the GRadient Ascent Pulse Engineering (GRAPE) technique [17] and had fidelities better than 0.999.

With our choice of measurement model (Fig. 1) we find a striking agreement with theoretical results for TTJP (19). One could have also run the postmeasured state resulting after the first dashed block in Fig. 1 through an arbitrary Completely Positive (CP) map before the next step. However, such a postprocessing CP map would have affected the results. In other words, our measurement scheme provides an optimal procedure to preserve the state information, thus resulting in an excellent agreement of experimental results for TTJP with theoretical prediction (see Fig. 5).

To calculate the moments we utilize the Moussa protocol [6], which requires only two spins in our case. We utilize $F_1$ as the system and $F_2$ as the ancilla qubit. $F_3$ was decoupled using $\pi$ pulses, and the initialization involved preparing the state $\frac{1-\epsilon}{8}\mathbb{1} + \epsilon\{\frac{1}{2}\mathbb{1}_S \otimes |+\rangle\langle +|_A \otimes |0\rangle\langle 0|\}$, which is obtained by applying the Hadamard gate to $F_2$ after the pulse sequence shown in Fig. 2(c). The circuit for measuring moments by the Moussa protocol is shown in Fig. 3, and it proceeds as follows:

$$
\begin{gathered}
\hat{\rho} \otimes |+\rangle\langle +| \\
\downarrow \mathrm{c}\hat{X}_1 \\
\hat{\rho}\hat{X}_1^\dagger \otimes |0\rangle\langle 1| + \hat{X}_1\hat{\rho} \otimes |1\rangle\langle 0| \\
+\hat{\rho} \otimes |0\rangle\langle 0| + \hat{X}_1\hat{\rho}\hat{X}_1^\dagger \otimes |1\rangle\langle 1|
\end{gathered}
$$

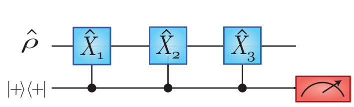


FIG. 3. (Color online) Moussa protocol for obtaining the three-time correlated moments. One- and two-time moments can be calculated using the appropriate number of controlled gates.

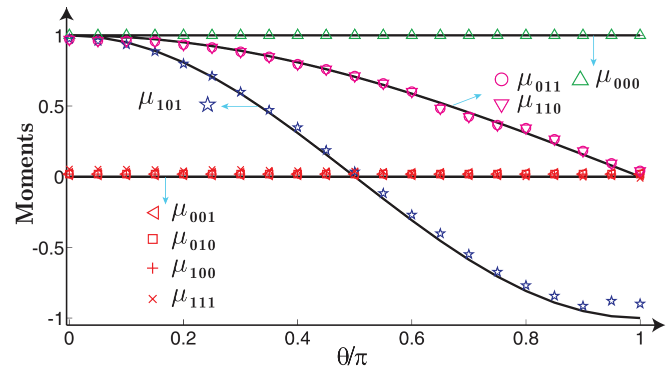


FIG. 4. (Color online) Moments obtained experimentally from the Moussa protocol. The symbols represent experimentally obtained values of the indicated moments, with the solid lines showing the corresponding theoretical values.

$$
\begin{gathered}
\downarrow \mathrm{c}\hat{X}_2 \\
\hat{\rho}\hat{X}_1^\dagger\hat{X}_2^\dagger \otimes |0\rangle\langle 1| + \hat{X}_2\hat{X}_1\hat{\rho} \otimes |1\rangle\langle 0| \\
+\hat{\rho} \otimes |0\rangle\langle 0| + \hat{X}_2\hat{X}_1\rho\hat{X}_1^\dagger\hat{X}_2^\dagger \otimes |1\rangle\langle 1| \\
\downarrow \mathrm{c}\hat{X}_3 \\
\hat{\rho}\hat{X}_1^\dagger\hat{X}_2^\dagger\hat{X}_3^\dagger \otimes |0\rangle\langle 1| + \hat{X}_3\hat{X}_2\hat{X}_1\hat{\rho} \otimes |1\rangle\langle 0| \\
+\hat{\rho} \otimes |0\rangle\langle 0| + \hat{X}_3\hat{X}_2\hat{X}_1\hat{\rho}\hat{X}_1^\dagger\hat{X}_2^\dagger\hat{X}_3^\dagger \otimes |1\rangle\langle 1|,
\end{gathered}
$$

where $\mathrm{c}\hat{X}_i$ represents the controlled gates and $\hat{\rho}$ is the initial state of the system. The state of the ancilla qubit $\hat{\rho}_a$ at the end of the circuit is given by

$$
\begin{aligned}
\hat{\rho}_a = {} & |0\rangle\langle 1|\mathrm{Tr}(\hat{\rho}\hat{X}_1^\dagger\hat{X}_2^\dagger\hat{X}_3^\dagger) + |1\rangle\langle 0|\mathrm{Tr}(\hat{X}_3\hat{X}_2\hat{X}_1\hat{\rho}) \\
& + |0\rangle\langle 0|\mathrm{Tr}(\hat{\rho}) + |1\rangle\langle 1|\mathrm{Tr}(\hat{X}_3\hat{X}_2\hat{X}_1\hat{\rho}\hat{X}_1^\dagger\hat{X}_2^\dagger\hat{X}_3^\dagger).
\end{aligned}
$$

The Moussa protocol was originally proposed for commutating observables; however, it can easily be extended to noncommutating observables. The NMR measurements correspond to the expectation values of spin angular momentum operators $I_x$ and $I_y$ [18]. The measurement of $I_x$ for the ancilla qubit at the end of the circuit gives

$$
\mathrm{Tr}[\hat{\rho}_a I_x] = \mathrm{Tr}[\hat{X}_3\hat{X}_2\hat{X}_1\hat{\rho}]/2 + \mathrm{Tr}[\hat{\rho}\hat{X}_1^\dagger\hat{X}_2^\dagger\hat{X}_3^\dagger]/2. \quad (20)
$$

If $\hat{X}_1, \hat{X}_2, \hat{X}_3$ commute, then the above expression gives $\mathrm{Tr}[\hat{\rho}\hat{X}_1\hat{X}_2\hat{X}_3]$. In the case of noncommuting Hermitian observables, we also measure the expectation value of $I_y$, which gives

$$
i\mathrm{Tr}[\rho_a I_y] = \mathrm{Tr}[\hat{X}_3\hat{X}_2\hat{X}_1\hat{\rho}]/2 - \mathrm{Tr}[\hat{\rho}\hat{X}_1^\dagger\hat{X}_2^\dagger\hat{X}_3^\dagger]/2. \quad (21)
$$

From (20) and (21) we can calculate $\mathrm{Tr}[\hat{\rho}\hat{X}_1\hat{X}_2\hat{X}_3] \equiv \langle\hat{X}_1\hat{X}_2\hat{X}_3\rangle$ for the three-measurement case. Hence, by using the different numbers of controlled gates in the appropriate order we can calculate all the moments. The experimentally obtained moments are shown in Fig. 4.

These experimentally obtained moments are inverted according to Eq. (4) to calculate the TTJP and are plotted along with the directly obtained TTJP using the circuit shown in Fig. 1 as symbols in Fig. 5. The theoretical values for TTJP from moments and the one directly obtained are plotted as solid and dashed lines, respectively. The results agree with the predictions of Eqs. (18) and (19) that the TTJP obtained

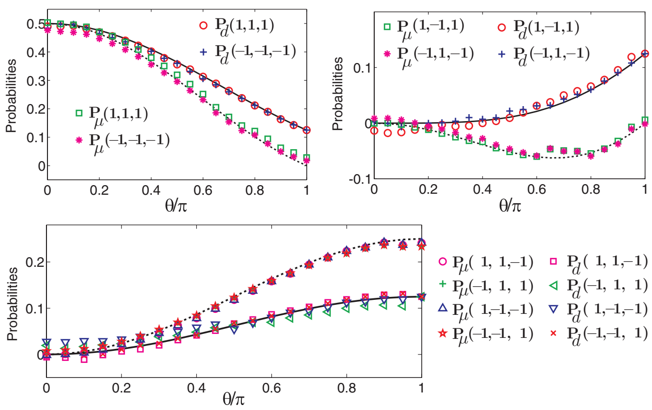


FIG. 5. (Color online) Three-time joint probabilities. The solid curve represents the probabilities obtained directly, and the dashed curve shows the probabilities obtained by inverting the moments. The symbols represent the experimental data.

directly and the one obtained from the inversion of moments do not agree.

## V. CONCLUSION

In the classical probability setting, statistical moments associated with dichotomic random variables determine the probabilities uniquely. When the same issue is explored in the quantum context, with random variables replaced by Hermitian observables (which are, in general, noncommuting), and the statistical outcomes of observables in sequential measurements are considered, it is shown that the joint probabilities do not agree with the ones inverted from the moments. This is explicitly illustrated by considering sequential measurements of a dynamical variable at three different times in the specific example of a spin-$1/2$ system. An experimental investigation based on NMR methods, where moments and joint probabilities are extracted independently, demonstrates the moment indeterminacy of probabilities, concordant with theoretical observations.

The failure to revert the joint probability distribution from its moments points towards its inherent incompatibility with the family of all marginals. In turn, the moment indeterminacy reveals the absence of a legitimate joint probability distribution compatible with the set of all marginal distributions, a common underpinning of various no-go theorems in the foundational aspects of quantum theory.

## ACKNOWLEDGMENTS

The authors are grateful to K. R. Koteswara Rao and Sudha for discussions. This work was partly supported by DST Project SR/S2/LOP-0017/2009.

[1] J. A. Shohat and J. D. Tamarkin, *The Problem of Moments* (American Mathematical Society, New York, 1943).
[2] N. I. Akhiezer, *The Classical Moment Problem* (Hafner, New York, 1965).
[3] A. N. Shiryaev, *Probability* (Springer, New York, 1996).
[4] The normalization condition $\sum_{q_1,q_2,\ldots,q_k=\pm1} P(q_1,q_2,\ldots,q_k) = 1$ is reflected in the zeroth-order moment $\mu_{00\cdots0} = 1$.
[5] H. Katiyar, A. Shukla, K. R. K. Rao, and T. S. Mahesh, Phys. Rev. A **87**, 052102 (2013).
[6] O. Moussa, C. A. Ryan, D. G. Cory, and R. Laflamme, Phys. Rev. Lett. **104**, 160501 (2010).
[7] A. Fine, Phys. Rev. Lett. **48**, 291 (1982).
[8] J. S. Bell, Rev. Mod. Phys. **38**, 447 (1966).
[9] S. Kochen and E. P. Specker, J. Math. Mech. **17**, 59 (1967).
[10] A. Peres, J. Phys. A **24**, L175 (1991).
[11] N. D. Mermin, Phys. Rev. Lett. **65**, 3373 (1990).
[12] A. J. Leggett and A. Garg, Phys. Rev. Lett. **54**, 857 (1985).
[13] A. R. Usha Devi, H. S. Karthik, Sudha, and A. K. Rajagopal, Phys. Rev. A **87**, 052103 (2013).
[14] M. Markiewicz, P. Kurzynski, J. Thompson, S. Y. Lee, A. Soeda, T. Paterek, and D. Kaszlikowski, arXiv:1302.3502.
[15] G. C. Knee *et al.*, Nat. Commun. **3**, 606 (2012).
[16] D. G. Cory, M. D. Price, and T. F. Havel, Phys. D **120**, 82 (1998).
[17] N. Khaneja, T. Reiss, C. Kehlet, T. Schulte-Herbrüggen, and S. J. Glaser, J. Magn. Reson. **172**, 296 (2005).
[18] J. Cavanagh, W. J. Fairbrother, A. G. Palmer, III, and N. J. Skelton, *Protein NMR Spectroscopy: Principles and Practice* (Academic Press, San Diego, 1995).